

8-2010

Multifunctional calcium carbonate microparticles: Synthesis and biological applications

Yu-Ho Won

Purdue University - Main Campus, ywon@purdue.edu

Ho Seong Jang

Purdue University - Main Campus, msekorea@purdue.edu

Ding-Wen Chung

Purdue University - Main Campus, dchung@purdue.edu

L Stanciu

Birck Nanotechnology Center and School of Materials Engineering, Purdue University, lstanciu@purdue.edu

Follow this and additional works at: <http://docs.lib.purdue.edu/nanopub>



Part of the [Nanoscience and Nanotechnology Commons](#)

Won, Yu-Ho; Jang, Ho Seong; Chung, Ding-Wen; and Stanciu, L, "Multifunctional calcium carbonate microparticles: Synthesis and biological applications" (2010). *Birck and NCN Publications*. Paper 622.

<http://docs.lib.purdue.edu/nanopub/622>

This document has been made available through Purdue e-Pubs, a service of the Purdue University Libraries. Please contact epubs@purdue.edu for additional information.

Multifunctional calcium carbonate microparticles: Synthesis and biological applications†

Yu-Ho Won,^{*a} Ho Seong Jang,^c Ding-Wen Chung^a and Lia A. Stanciu^{ab}

Received 28th April 2010, Accepted 1st July 2010

DOI: 10.1039/c0jm01231a

Multifunctional composites based on calcium carbonate (CaCO₃) spherical microparticles stabilized through the embedding of CdSe/ZnS/SiO₂ nanoparticles into surface pores were fabricated. The stabilization of the vaterite polymorph of CaCO₃ through nanoparticles embedding was necessary to generate a spherical, porous morphology of the microparticles. The CdSe/ZnS quantum dots were obtained and dispersed in aqueous solution after coating them with a silica shell *via* a reverse microemulsion approach. Green and red-emitting CaCO₃-CdSe/ZnS/SiO₂ microcomposites were analyzed *via* confocal laser-scanning fluorescence microscopy to demonstrate their potential for imaging applications. The acetylcholinesterase (AChE) enzyme was immobilized into the pores of the spherical CaCO₃-CdSe/ZnS/SiO₂ microcomposites and the resulting hybrid material was used as a platform for the design of a pesticide biosensor. The detection limit for the paraoxon pesticide in aqueous solutions was determined to be of 4.6 nM.

1. Introduction

Recently, composite nano and microstructured materials consisting of more than two different materials have been studied extensively because of their potential to combine the different properties of the individual component materials, resulting in multifunctionality and versatility. Quantum dots (QDs), having superior optical properties such as size-tunable light emission, narrow emission band width, broad excitation band, and high photostability are one category of such materials with properties that makes them attractive for the design of composite materials with multiple functionality.¹ QDs have been widely used for biological applications such as biolabeling,¹ imaging,² optical encoding,³ or biosensing.⁴ Among several QDs, CdSe based QDs have attracted considerable attention because they cover the entire visible region, from blue to red, and have high quantum efficiency.⁵ Core/shell structured QDs with wide bandgap semiconductor shells have been developed to further improve their stability and quantum efficiency.⁶ CdSe/ZnS core/shell QDs with high quantum efficiency were reported by Dabbousi *et al.*⁶ For biological applications, the surface of QDs synthesized *via* an organometallic based approach requires modification due to its hydrophobicity that renders the QDs unusable in aqueous media. Several approaches to achieve QDs with hydrophilic surface properties have been reported including ligand exchange,⁷ amphiphilic polymer modification,⁸ and silica (SiO₂) shell formation.⁹ Silica shell formation is an attractive surface

modification method for water soluble QDs for biological applications, due to the optical transparency and biocompatibility of silica.¹⁰ In addition, the surface of the silica shell is chemically reactive and can be therefore easily modified with additional functional groups by conventional surface chemistry.¹¹ The reverse microemulsion method for silica shell formation on QDs was used by several groups, who used Igepal CO-520 as a surfactant, hexane as a hydrophobic solvent, and tetraethyl orthosilicate (TEOS) as a precursor of silica.^{9,12}

Calcium carbonate is one of the main biomineral components of seashells. It is fascinating how nature skillfully designs and precisely controls the architecture, polymorphism, chemical composition and morphology of such biominerals. The polymorph control of calcium carbonate biomineral in seashells is achieved naturally by complex cellular cues. Calcium carbonate has three different crystalline forms, such as vaterite, calcite and aragonite. The porous CaCO₃ microspheres can be an effective host for the fabrication of biocompatible composite materials due to its availability in nature as a biomineral and its porous structure that is suitable for loading other materials.¹³ These characteristics lead to CaCO₃ microspheres being used for drug delivery,¹⁴ biosensing,^{13,15} and protein encapsulation.¹⁶ The difficulty in using this attractive material for the design of multifunctional composites stays in its polymorphic character. The most attractive phase of CaCO₃ as a matrix for the fabrication of multifunctional materials, featuring a spherical morphology and porous surface is the metastable vaterite form. Vaterite easily undergoes the phase transition to the more thermodynamically stable phase of CaCO₃, calcite, which does not however present with the spherical porous morphology of vaterite.¹⁶ This phase transformation usually occurs overnight for vaterite samples kept in DI water.¹⁶ Stabilization of the vaterite form of CaCO₃ can be achieved *via* presence of impurities of inorganic or organic materials.^{17,18} To stabilize the vaterite phase, several research groups used organic impurities such as ovalbumin,¹⁸ polypeptide,¹⁹ double hydrophilic block

^aSchool of Materials Engineering, Purdue University, West Lafayette, Indiana, 47907, USA. E-mail: ywon@purdue.edu; Fax: +1-765-494-1204; Tel: +1-765-337-5177

^bBirk Nanotechnology center, Purdue University, West Lafayette, Indiana, 47907, USA

^cDepartment of Chemistry, Purdue University, West Lafayette, Indiana, 47907, USA

† Electronic supplementary information (ESI) available: Supplementary Fig. S1–S3 and Table S1. See DOI: 10.1039/c0jm01231a

copolymers,²⁰ and anionic starburst dendrimer.²¹ Cai *et al.* embedded gold nanoparticles (NPs) into the pores of CaCO₃.¹⁵ For the same stabilization purposes, Wang *et al.* used a layer-by-layer approach and deposited polyelectrolyte multilayer films on the vaterite surface.¹⁴ The vaterite polymorph can be stabilized for more than a year through some of these stabilization methods.²⁰ In this work, we report on using, for the first time, both pore embedding of CdSe/ZnS/SiO₂ NPs and coating of the vaterite phase with polyethylene glycol (PEG) to stabilize the vaterite form of CaCO₃ with a microspherical, porous structure. By doing so, CdSe/ZnS/SiO₂ NPs can act as both a vaterite stabilizer and at the same time add functionality to the microspheres to be potentially used as fluorescent probes. The PEG layer can have both a vaterite stabilizing effect and provide added chemical activity for further modification with functional molecules. By combining these approaches, in this work we demonstrate the synthesis of novel microcomposites with multifunctional properties, consisting of porous CaCO₃ and CdSe/ZnS/SiO₂ NPs and describe their potential applications as fluorescent probes for imaging and as biosensing platform materials after modification with a model enzyme, acetylcholinesterase (AChE).

2. Experimental

2.1. Materials

CaCl₂·H₂O and Na₂CO₃ were obtained from Sigma Aldrich to prepare CaCO₃ microspheres. In order to synthesize CdSe/ZnS QDs, cadmium acetate dihydrate (Cd(CH₃COO)₂·2H₂O), selenium powder, zinc acetate, bis(trimethylsilyl) sulfide, trioctylphosphine (TOP, technical grade), trioctylphosphine-oxide (TOPO, technical grade), hexadecylamine (HDA, technical grade), hexane, and ethanol were purchased from Sigma Adrich. IGEPAL CO-520, ammonium hydroxide (NH₄OH), tetraethyl orthosilicate (TEOS), and methanol were obtained from Sigma Adrich for silica shell formation on CdSe/ZnS QDs. To test the pesticide biosensor, acetylcholinesterase (AChE), acetylthiocholine chloride (ATChCl), polyethylene glycol (PEG), paraoxon, and phosphate buffered saline (PBS, pH 7.4) were purchased from Sigma Adrich. All chemicals were used without additional purification.

2.2. Synthesis of CaCO₃-CdSe/ZnS/SiO₂ microcomposites

Porous CaCO₃ microspheres were prepared *via* the process reported by Volodkin *et al.*^{16,22} 0.33 M Na₂CO₃ and 0.33 M CaCl₂·H₂O solution were prepared with 10 ml deionized (DI) water. The Na₂CO₃ solution was poured into CaCl₂·H₂O solution and the mixture was stirred for 10 min. The mixture was centrifuged and washed with DI water, and then dried in air.

CdSe QDs and CdSe/ZnS QDs are synthesized by using organometallic based thermal decomposition method.^{23,24} In order to synthesize CdSe QDs, TOP-Se was prepared through heating TOP (12.5 ml) and selenium powder (1.5 g) to 230 °C for 20 min under argon gas as first step. Then, cadmium acetate dehydrate (0.054 g), TOPO (4 g), and HDA (2 g) were added to 50 ml three-neck flask. The mixture was heated to 300 °C under argon gas and TOP-Se (2 ml) which was prepared separately was quickly added into the flask. The color of the solution was

changed from yellow to deep brown with increasing growth time. CdSe QDs of different sizes were obtained by controlling the growth time. The solution was cooled down to room temperature by adding hexane and washed through precipitation and centrifugation by ethanol. Finally, CdSe QDs were dispersed in hydrophobic solvent such as hexane.

To make ZnS shell on the CdSe, TOP-Zn and TOP-S were prepared by the same method as the formation of TOP-Se. CdSe QDs, TOPO, and HDA were heated to 150 °C in 50 ml three-neck flask. TOP-Zn and TOP-S were added into the flask by syringe pump (30 µl/min). The mixture was kept to 150 °C for 12 h to improve the crystallinity of ZnS shell.

Silica shell was formed on CdSe/ZnS QDs to make them dispersed in aqueous solution for biology applications by reverse microemulsion approach.^{9,12} CdSe/ZnS QDs (1 ml) were added into the flask with hexane (7 ml), Igepal CO-520 (0.6 ml), and ammonium hydroxide (0.1 ml). TEOS as a precursor of silica shell was added into the flask and the mixture was stirred for 20 h. The solution was precipitated by methanol and centrifuged and CdSe/ZnS/SiO₂ NPs were finally dispersed in DI water.

In order to prepare microcomposites consist of CaCO₃ and CdSe/ZnS/SiO₂ NPs, 2 mg CaCO₃ particles dispersed in 1 ml DI water and 0.2 ml CdSe/ZnS/SiO₂ NPs (0.8 mg/ml) were added into the solution. The mixture was stirred for 30 min and centrifuged to remove CdSe/ZnS/SiO₂ NPs which were not attached on CaCO₃.

2.3. Fabrication of pesticide-biosensors

To apply the synthesized microcomposites to pesticide biosensor fabrication, AChE enzymes were immobilized into CaCO₃-CdSe/ZnS/SiO₂ microcomposites. 100 µl AChE enzymes solution which were prepared in PBS (pH 7.4) and 20 µl PEG were added into 100 µl CaCO₃-CdSe/ZnS/SiO₂ microcomposites solution and the solution was stirred for 2 h to incubate enzymes under 4 °C. Then, the mixture (3 µl) was deposited on the screen printed electrodes (SPEs, Pine Research Instrumentation) and dried overnight. The SPEs were stored in PBS under 4 °C.

2.4. Characterization

Synthesized CaCO₃ and CdSe/ZnS/SiO₂ NPs were characterized by scanning electron microscopy (SEM, Nova NanoSEM 200 (FEI Company, USA)) operated at 10 kV and transmission electron microscopy (TEM, Tecnai 20 (FEI Company, USA)) operated at 200 kV. The X-ray diffraction pattern of the CaCO₃ was measured with a Bruker D8 focus (Cu K α , λ = 1.5406 Å). The ultraviolet-visible (UV-vis) absorption spectra were recorded using SpectraMax Plus spectrometer (Molecular devices, USA). Confocal fluorescent microscopy images of CaCO₃-CdSe/ZnS/SiO₂ microcomposites were obtained by FV1000 + IX81 laser-scanning microscope (Olympus America Inc., PA) with femto second laser source (Mai Tai, Spectra-Physics, Fremont, CA). The biosensors were tested at room temperature using BASi epsilon C3 cell stand by a method previously reported by our group.¹²

3. Results and discussion

3.1. Synthesis and characterization of porous CaCO_3

The spherical, porous, vaterite form of CaCO_3 was synthesized by mixing 0.33 M Na_2CO_3 and 0.33 M $\text{CaCl}_2 \cdot \text{H}_2\text{O}$ solution.^{16,22} Fig. 1 shows SEM images of porous CaCO_3 microspheres composed of individual, smaller CaCO_3 NPs (10 ~ 30 nm).¹³ The microspheres are uniform with 3 ~ 5 μm and well dispersed in deionized (DI) water as shown in Fig. 1a. From Fig. 1b, the high magnification SEM image, it is confirmed that the microsphere has a porous surface, with 20–60 nm pore sizes.^{16,22} In order to confirm the phase of the CaCO_3 microspheres, an XRD pattern was obtained from the synthesized CaCO_3 powder, after drying in air. The XRD pattern is consistent with the vaterite phase of CaCO_3 (JPCDS #: 24-0030) as shown in Fig. 2. There are a few low intensity peaks corresponding to the calcite phase. This indicates that a small amount of calcite phase coexists with the vaterite phase. Calcite being the most thermodynamically stable form of calcium carbonate at room temperature and under ambient pressure, it is not surprising to find the presence of the residual calcite phase. However, the complete vaterite-calcite transformation that usually occurs under ambient conditions can be significantly slowed down by impeding the face growth of the vaterite crystals and transformation of the hexagonal crystal structure of vaterite to the rhombohedral crystal structure of calcite. However, immediately after vaterite synthesis, the low intensity of the calcite phase XRD peaks, coupled with the low

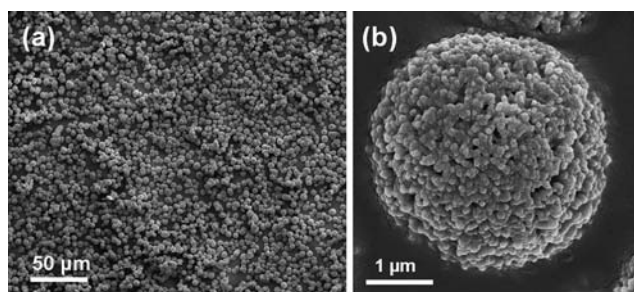


Fig. 1 SEM images of synthesized porous CaCO_3 particles with (a) low magnification and (b) high magnification.

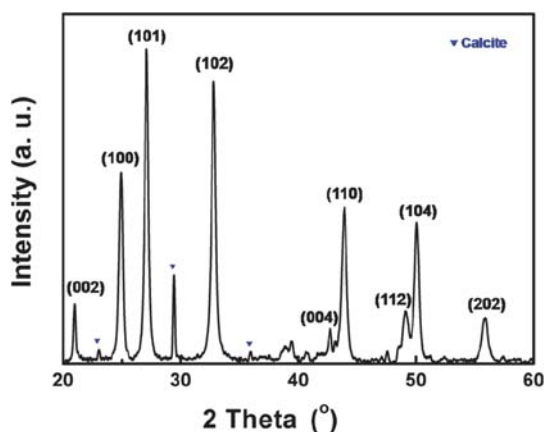


Fig. 2 XRD pattern of synthesized porous CaCO_3 particles with vaterite phase (\blacktriangledown : calcite phase).

magnification SEM observations that indicated that the rectangular morphology of calcite is very sparsely present in the samples, make us confident that the spherical, porous morphology of the vaterite phase is predominant enough to make this material useful for various applications if the phase transformation is stopped through means of stabilization that will be discussed in section 2.3.

3.2. Synthesis and characterization of CdSe/ZnS/SiO_2

Due to the quantum confinement effect, CdSe QDs can emit light with different wavelength in the visible spectrum, depending on their size. The size of CdSe QDs can be easily tuned by changing the growth time during synthesis. For this work, ZnS ($E_g = 3.66$ eV at 300 K), which has a wider bandgap than that of CdSe ($E_g = 1.74$ eV at 300 K) was selected as a shell material for the fabrication of CdSe/ZnS core-shell nanoparticles. Covering CdSe QDs with a ZnS layer improves the stability and quantum yield. Figs. S1a and S1b (ESI†) show representative TEM images of red-emitting CdSe QDs and CdSe/ZnS QDs. The CdSe/ZnS QDs are uniform in size (~ 4.5 nm) and well dispersed and arrayed. Figs. S1c and S1d (ESI†) are UV-vis absorption spectra and digital camera images of CdSe QDs with different sizes under 365 nm UV lamp. The absorption bands were shifted to longer wavelengths as the size of CdSe QDs increased. This demonstrates that the bandgap energy of the QDs decreases as their size increases. The digital camera images show the emitting color variation of the QDs with increasing their size (Fig. S1d, Supporting Information†).

The properties of CdSe/ZnS QDs render these materials amenable to surface modification. For applications in biological fields, using a silica shell on the surface of CdSe/Zn QDs may be appropriate due to its biocompatibility and dispersability in DI water.¹⁰ A silica shell was formed on the CdSe/ZnS QDs, by using a reverse microemulsion approach.^{9,12} Fig. 3 shows TEM and SEM images of CdSe/ZnS/SiO₂ NPs with various sizes, respectively. In the Fig. 3a and 3d, the CdSe/ZnS/SiO₂ NPs are about 25 nm in diameter and are composed of red-emitting CdSe/ZnS QD of about 4.5 ~ 5 nm diameter and a silica shell of about 10 nm in thickness. In addition, the size of the NPs can be simply controlled by the modification of the silica shell thickness which can be changed concentration of a precursor of silica, TEOS. The diameters of CdSe/ZnS/SiO₂ NPs were increased as concentration of TEOS increased. As shown in Fig. 3b~3f (TEM and SEM images), diameters of CdSe/ZnS/SiO₂ NPs are 40 (b,e) and 85 nm (c,f) with silica shell 17.5 and 40 nm thicknesses, respectively.

3.3. Stabilization of vaterite and multicomposite fabrication and characterization

In order to stabilize the vaterite phase and at the same time create a multifunctional composite, CdSe/ZnS/SiO₂ NPs were conjugated into the surface pores of CaCO_3 microspheres.¹⁵ CdSe/ZnS/SiO₂ NPs of 25 nm diameter were used due to their size matching the pore sizes of CaCO_3 , which are ~ 20 to 60 nm. Since the isoelectric points of CaCO_3 and CdSe/ZnS/SiO₂ NPs are 8.5¹⁵ and 2 ~ 3,²⁵ respectively, the negatively charged CdSe/ZnS/SiO₂ NPs are conjugated into the pores of positively charged CaCO_3 microparticles at neutral pH by electrostatic interaction. Previous

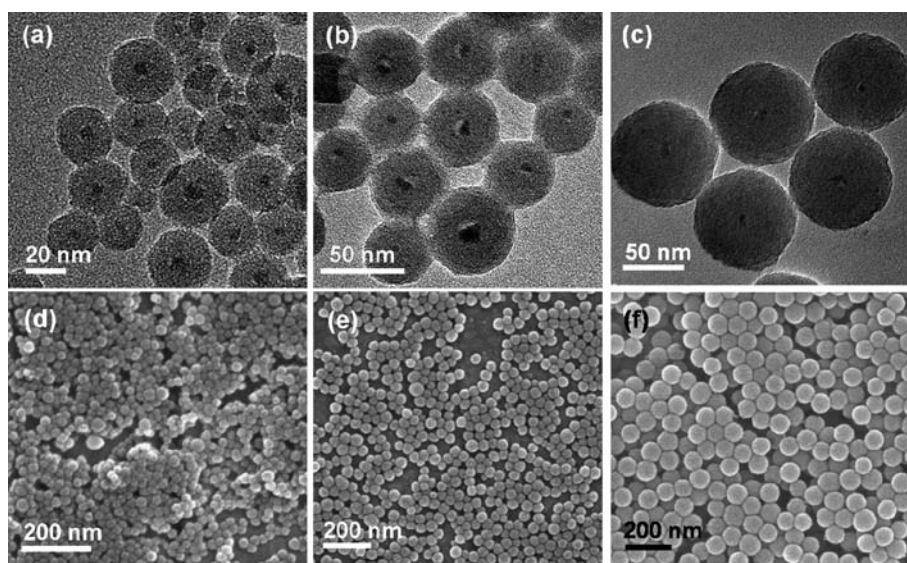


Fig. 3 TEM and SEM images of (a),(d) 25 nm, (b),(e) 40 nm, (c),(f) 85 nm CdSe/ZnS/SiO₂ core/shell/shell NPs.

research showed that coupling vaterite with inorganic materials leads to the formation of solid solutions between calcium carbonate and these inorganic materials on the vaterite surface.²⁶ These solid solutions have been shown to have a lower heat of formation than that of calcite, thus preventing the dissolution of the vaterite polymorph. Although different chemistries of both inorganic and organic stabilizers have been proposed by others,^{15,18–21,26} we speculate that similar stabilizing mechanisms, with the formation of thermodynamically stable compounds (with heat of formation lower than that of calcite) between the stabilizer and the calcium carbonate, at the microparticle surface is acting in the case of our proposed stabilizing materials.

Fig. 4a–4f show SEM images of CaCO₃ (a,d), CaCO₃-CdSe/ZnS/SiO₂ (b,e), and PEG-AChE-CaCO₃-CdSe/ZnS/SiO₂ (c,f),

respectively. Fig. 4b and 4e show that CdSe/ZnS/SiO₂ NPs are present into the pores on the CaCO₃ microspheres and they kept the morphology of the vaterite phase after conjugation. Fig. S2 (ESI[†]) shows SEM images of spherical CaCO₃-CdSe/ZnS/SiO₂ microcomposites, indicating a vaterite morphology.

This multifunctional microcomposite has the potential to be used for bioimaging applications due to the optical properties of CdSe/ZnS QDs and the biocompatibility properties of CaCO₃ and SiO₂. Another stabilizer of the vaterite structure, PEG, was added on the surface of the calcium carbonate microcomposites that also provided additional chemical reactivity for coupling of biologicals. As an example of the applicability of this material platform for biosensor design, the AChE enzyme was chosen as a model enzyme and immobilized onto the microcomposite

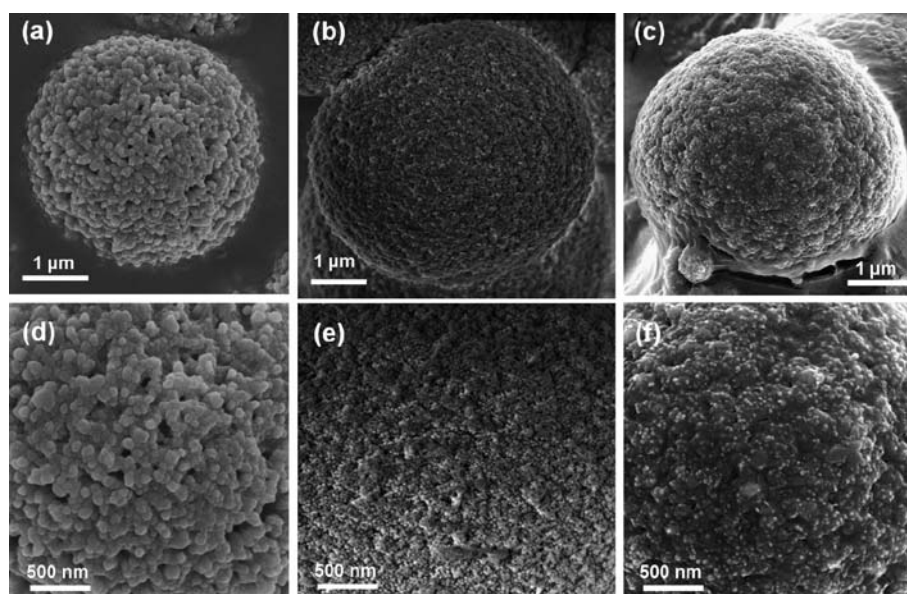


Fig. 4 SEM images of (a),(d) CaCO₃, (b),(e) CaCO₃-CdSe/ZnS/SiO₂ NPs, and (c),(f) PEG-AChE-CaCO₃-CdSe/ZnS/SiO₂ microcomposites.

surface by covalent binding to PEG.²⁷ In addition to the enzymatic stabilization effect that the PEG has, the isoelectric points of CaCO₃ and AChE are 8.5¹⁵ and 5.5,²⁸ respectively. Thus, the electrostatic interaction between CaCO₃ and AChE is also favorable, since at a neutral pH that was used in these experiments, CaCO₃ is positively charged, while AChE is negatively charged. From the SEM images in Fig. 4c and 4f, it is apparent that the size of the pores of the microcomposites decreased following AChE immobilization.²⁹

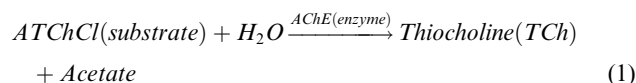
3.4. Imaging and biosensing capabilities of CaCO₃-CdSe/ZnS/SiO₂ microcomposites

CaCO₃-CdSe/ZnS/SiO₂ microcomposites were tested for potential applications in two different fields, imaging and biosensing. As mentioned earlier, due to the biocompatibility and water solubility of both calcium carbonate and silica, the synthesized microcomposites have the potential to find biological applications. Confocal fluorescent microscopy images of the green and red-emitting CaCO₃-CdSe/ZnS/SiO₂ microcomposites were obtained to show the potential for imaging applications (Fig. 5). The excitation source was 488 nm laser and two types of filters were used, 505–535 nm and 581–608 nm for the microcomposites containing green (Fig. 5a) and red-emitting QDs (Fig. 5b), respectively. The confocal fluorescent microscopy images were overlapped with transmitted images of the microcomposites and the insets are fluorescence images of CdSe/ZnS QDs under 365 nm UV lamp. The green and red fluorescence were observed on the location of the microcomposites. These results demonstrate that the fluorescence properties of CdSe/ZnS QDs in the microcomposites has the potential to be applied to imaging of biomolecules such as proteins or cells.

To test the potential of the CaCO₃-CdSe/ZnS/SiO₂ microcomposites as materials for biosensor platforms, AChE enzyme was chosen as a model enzyme and immobilized on their surface. Among various detection methods of biosensors, an amperometric approach has several advantages such as rapid response, superior sensitivity, simplicity, relatively low cost, and so on.³⁰ Therefore, an amperometric method was used for the fabrication of a pesticide biosensor using PEG-AChE-CaCO₃-CdSe/ZnS/SiO₂ microcomposites as an electrode material. For the immobilization of AChE, 100 μ l AChE solution (PBS, pH 7.4) and 20 μ l PEG (20% v/v in DI water) was incubated with 100 μ l CaCO₃-CdSe/ZnS/SiO₂ microcomposites for two hours. The resulted hybrid enzyme-microparticle composites (3 μ l) were

deposited on the screen printed electrodes (SPEs) with the working electrode area of 4 \times 5 mm², which were pretreated to render their surface hydrophilic by direct current (DC) potential amperometry (1750 mV vs. Ag/AgCl) for 5 min and dried overnight in air. The surface area of the SPE after surface modification is calculated to be 31.42 mm². For this calculation we assumed the microparticles are uniform spheres with 4 μ m in diameter and one layer coating on the SPE. The SPEs were stored in 3 ml phosphate buffered saline (PBS, pH 7.4) at 4 $^{\circ}$ C before use.

ATChCl is generally used as a substrate for AChE based amperometric biosensors. The reaction mechanism is as shown in eqn (1),¹²



ATChCl is hydrolyzed to TCh and acetate by AChE and TCh is changed to dithio-bis-choline. From the cyclic voltammetry curves (Fig. S3a, ESI[†]), the oxidation peak of ATChCl is located at 250 mV. The current response of SPEs with microcomposites was saturated at a substrate concentration of 1.0 mM ATChCl (Fig. S3b, ESI[†]). In order to find the optimum conditions for the biosensor, both the concentration of AChE and the pH of the measuring solution were optimized (Fig. S3c and S3d, ESI[†]). The current response was saturated at 23.8 mU AChE and reached maximum point at pH 7.4 PBS solution. Thus, the applied potential, ATChCl and AChE concentration, and pH value of measuring solution were set to 250 mV, 1.0 mM, 23.8 mU, and 7.4 for further biosensor tests. The inhibition curve of the biosensor was obtained by using paraoxon, an organophosphorous pesticide. Six SPEs were prepared by coating them with the hybrid microcomposites. Fig. 6a shows the calibration curve of six SPEs. Their current responses have a 10% standard deviation at 1.0 mM ATChCl. To determine the concentration of paraoxon, each SPE was incubated in a paraoxon solution of different concentration. After incubation for 10 min, the current response of SPEs were measured and the inhibition (%) was calculated by eqn (2):

$$\text{Inhibition (\%)} = 100 \times \frac{\text{Initial current} - \text{final current}}{\text{Initial current}} \quad (2)$$

The inhibition curve of the SPEs shows a linear relationship between inhibition (%) and paraoxon concentration as shown in Fig. 6b. The inhibition (%) of the biosensor is proportional to the paraoxon concentration in the range of from 4.6 nM to 46 μ M.

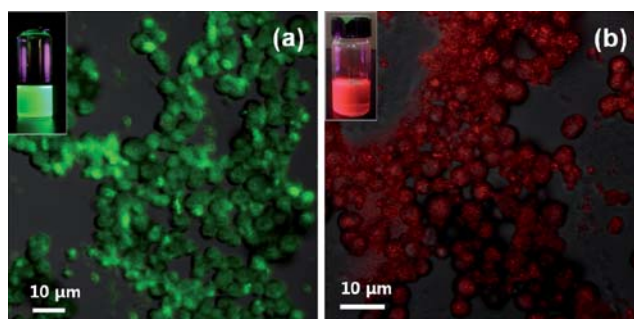


Fig. 5 Fluorescence microscopy images of CaCO₃-CdSe/ZnS/SiO₂ using (a) green emitting and (b) red emitting CdSe/ZnS QDs.

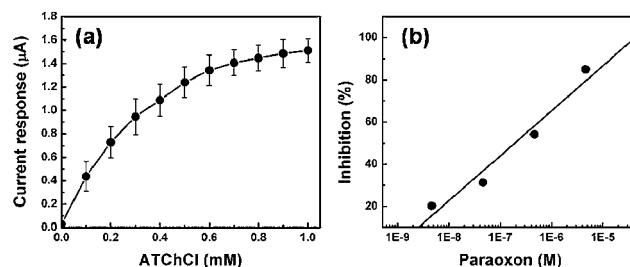


Fig. 6 (a) Calibration curve and (b) inhibition curve of paraoxon biosensor with PEG-AChE-CaCO₃-CdSe/ZnS/SiO₂ microcomposites.

Thus, the detection limit was determined to be 4.6 nM of paraoxon corresponding to 0.0013 ppm at an inhibition of 20% ($I_{20\%}$). Amperometric biosensors are more sensitive compared with other methods such as fluorescence spectroscopy and chromatography. The detection limit (4.6 nM of paraoxon) of the biosensor with PEG-AChE-CaCO₃-CdSe/ZnS/SiO₂ microcomposites lower when compared with other biosensors, shown in Table S1 (ESI†).^{31–35} The current United States Environmental Protection Agency (U.S. EPA) standards for organophosphate pesticides allow the presence of pesticides in concentrations varying in the range of 0.1 to 1 ppm. Therefore, we can confidently state that the fabricated paraoxon biosensor has a lower detection limit than the EPA standards. This demonstrates that the synthesized microcomposite shows great promise as a material platform candidate for electrochemical biosensors.

4. Conclusion

A novel multifunctional microcomposite, based on a porous CaCO₃ and CdSe/ZnS/SiO₂NPs, was fabricated. The vaterite polymorph of CaCO₃, which is good template for biological applications was stabilized with CdSe/ZnS/SiO₂ NPs and PEG layer. The multifunctional microcomposite have advantages of high surface area, high porosity, biocompatibility, and superior fluorescent properties. Based on these properties, the microcomposites were tested for their functionalities in imaging and biosensing. From confocal fluorescent spectroscopy images, we inferred that CaCO₃-CdSe/ZnS/SiO₂ demonstrated their potential as biomarkers. In addition, AChE enzyme immobilized CaCO₃-CdSe/ZnS/SiO₂ were tested to fabricate an amperometric pesticide biosensor as an example of potential applications in the biosensing and biocatalysis. The biosensor detection limit was of 10⁻⁹ M for paraoxon, which is lower than the value from U.S. EPA standards. Thus, CaCO₃-CdSe/ZnS/SiO₂ microcomposites showed their versatility and multifunctionality and the potential of being used for imaging as well as biosensing applications.

Acknowledgements

The authors are grateful for the financial support provided by NSF DMR #0804464 and NSF OISE#0728130 awards.

References

- X. H. Gao, Y. Y. Cui, R. M. Levenson, L. W. K. Chung and S. M. Nie, *Nat. Biotechnol.*, 2004, **22**, 969.
- I. L. Medintz, H. T. Uyeda, E. R. Goldman and H. Mattoussi, *Nat. Mater.*, 2005, **4**, 435.
- X. H. Gao and S. M. Nie, *J. Phys. Chem. B*, 2003, **107**, 11575.
- V. Pardo-Yissar, E. Katz, J. Wasserman and I. Willner, *J. Am. Chem. Soc.*, 2003, **125**, 622.
- C. B. Murray, D. J. Norris and M. G. Bawendi, *J. Am. Chem. Soc.*, 1993, **115**, 8706.
- B. O. Dabbousi, J. RodriguezViejo, F. V. Mikulec, J. R. Heine, H. Mattoussi, R. Ober, K. F. Jensen and M. G. Bawendi, *J. Phys. Chem. B*, 1997, **101**, 9463.
- X. Q. Wang, J. F. Wu, F. Y. Li and H. B. Li, *Nanotechnology*, 2008, **19**, 205501.
- D. R. Larson, W. R. Zipfel, R. M. Williams, S. W. Clark, M. P. Bruchez, F. W. Wise and W. W. Webb, *Science*, 2003, **300**, 1434.
- D. K. Yi, S. T. Selvan, S. S. Lee, G. C. Papaefthymiou, D. Kundaliya and J. Y. Ying, *J. Am. Chem. Soc.*, 2005, **127**, 4990.
- K. P. Velikov and A. van Blaaderen, *Langmuir*, 2001, **17**, 4779.
- A. L. Rogach, D. Nagesha, J. W. Ostrander, M. Giersig and N. A. Kotov, *Chem. Mater.*, 2000, **12**, 2676.
- Y. H. Won, H. S. Jang, S. M. Kim, E. Stach, M. Ganesana, S. Andreescu and L. A. Stanciu, *Langmuir*, 2010, **26**, 4320.
- W. Y. Cai, L. D. Feng, S. H. Liu and J. J. Zhu, *Adv. Funct. Mater.*, 2008, **18**, 3127.
- C. Y. Wang, C. Y. He, Z. Tong, X. X. Liu, B. Y. Ren and F. Zeng, *Int. J. Pharm.*, 2006, **308**, 160.
- W. Y. Cai, Q. Xu, X. N. Zhao, J. J. Zhu and H. Y. Chen, *Chem. Mater.*, 2006, **18**, 279.
- D. V. Volodkin, N. I. Larionova and G. B. Sukhorukov, *Biomacromolecules*, 2004, **5**, 1962.
- V. Nothig-Laslo and L. Brecevic, *Phys. Chem. Chem. Phys.*, 1999, **1**, 3697.
- X. Q. Wang, R. Kong, X. X. Pan, H. Xu, D. H. Xia, H. H. Shan and J. R. Lu, *J. Phys. Chem. B*, 2009, **113**, 8975.
- Z. P. Zhang, D. M. Gao, H. Zhao, C. G. Xie, G. J. Guan, D. P. Wang and S. H. Yu, *J. Phys. Chem. B*, 2006, **110**, 8613.
- H. Colfen and M. Antonietti, *Langmuir*, 1998, **14**, 582.
- K. Naka, Y. Tanaka and Y. Chujo, *Langmuir*, 2002, **18**, 3655.
- D. V. Volodkin, A. I. Petrov, M. Prevot and G. B. Sukhorukov, *Langmuir*, 2004, **20**, 3398.
- H. S. Jang, H. Yang, S. W. Kim, J. Y. Han, S. G. Lee and D. Y. Jeon, *Adv. Mater.*, 2008, **20**, 2696.
- H. S. Jang, B. H. Kwon, H. Yang and D. Y. Jeon, *Appl. Phys. Lett.*, 2009, **95**, 161901.
- L. Bergman, J. Rosenholm, A. B. Öst, A. Duchanoy, P. Kankaanpää, J. Heino and M. Lindén, *J. Nanomater.*, 2008, **2008**, 1.
- N. Nassrallah-Aboukais, A. Boughriet, J. Laureyns, L. Gengembre and A. Aboukais, *Chem. Mater.*, 1999, **11**, 44.
- R. Sinha, M. Ganesana, S. Andreescu and L. Stanciu, *Anal. Chim. Acta*, 2010, **661**, 195.
- J. W. Choi, J. H. Min, J. W. Jung, H. W. Rhee and W. H. Lee, *Thin Solid Films*, 1998, **327–329**, 676.
- A. A. Ansari, P. R. Solanki and B. D. Malhotra, *J. Biotechnol.*, 2009, **142**, 179.
- K. Thenmozhi and S. S. Narayanan, *Anal. Bioanal. Chem.*, 2007, **387**, 1075.
- M. Ramanathan and A. L. Simonian, *Biosens. Bioelectron.*, 2007, **22**, 3001.
- S. Paliwal, M. Wales, T. Good, J. Grimsley, J. Wild and A. Simonian, *Anal. Chim. Acta*, 2007, **596**, 9.
- A. L. Simonian, T. A. Good, S. Wang and J. R. Wild, *Anal. Chim. Acta*, 2005, **534**, 69.
- A. Di Corcia and M. Marchetti, *Anal. Chem.*, 1991, **63**, 580.
- L. Campanella, D. Lelo, E. Martini and M. Tomassetti, *Anal. Chim. Acta*, 2007, **587**, 22.